

Covert Wireless Communications with Channel Inversion Power Control in Rayleigh Fading

Jinsong Hu, *Student Member, IEEE*, Shihao Yan, *Member, IEEE*,
 Xiangyun Zhou, *Senior Member, IEEE*, Feng Shu, *Member, IEEE*,
 and Jun Li, *Senior Member, IEEE*

Abstract

Considering Rayleigh fading channels, in this work we adopt channel inversion power control to achieve covert communications, where a transmitter can possibly hide itself from a warden while transmitting information to a receiver. Specifically, we examine the performance of the achieved covert communications in two scenarios in terms of the effective covert rate (ECR), which quantifies the amount of information that the transmitter can reliably convey to the receiver subject to the warden's detection error probability being no less than some specific value. In the first scenario, the noise uncertainty at the warden serves as the enabler of covert communications and our examination shows that increasing the noise uncertainty at the warden and the receiver simultaneously may not continuously improve the ECR. In the second scenario, covert communications are aided by a full-duplex receiver, which always transmits artificial noise (AN) with a random power. Our analysis indicates that the achieved ECR approaches to an upper bound as the transmit power of AN approaches to infinity. This work provides

J. Hu, F. Shu, and J. Li are with the School of Electronic and Optical Engineering, Nanjing University of Science and Technology, Nanjing, China. (Emails: {jinsong_hu, shufeng, jun.li}@njust.edu.cn). J. Hu is also a visiting PhD student at the Research School of Engineering, Australian National University, Canberra, ACT, Australia. F. Shu is also with National Key Laboratory of Electromagnetic Environment, China Research Institute of Radiowave Propagation, China, and with National Mobile Communications Research Laboratory, Southeast University, Nanjing, China.

S. Yan is with the School of Engineering, Macquarie University, Sydney, NSW, Australia (Email: shihao.yan@mq.edu.au).

X. Zhou is with the Research School of Engineering, Australian National University, Canberra, ACT, Australia (Email:xiangyun.zhou@anu.edu.au).

This work was supported in part by the National Natural Science Foundation of China (Nos. 61472190, 61501238, 61727802, and 61771244), the Jiangsu Provincial Science Foundation Project (BK20150786), and the open research fund of National Mobile Communications Research Laboratory, Southeast University, China (No. 2017D04).

useful guidelines and performance limits on achieving covert communications and potentially hiding a transmitter in practical Rayleigh fading channels.

Index Terms

Physical layer security, covert communications, noise uncertainty, full duplex, artificial noise.

I. INTRODUCTION

With the ever-increasing use of the Internet of Things (IoT), various types of small devices are becoming part of the wireless connected world, whose overall goal is to improve the quality of our daily life. In a wide range of application scenarios, the security of IoT is a critical issue. For example, in health-care systems, some wireless sensors collect patients' health information such as heart rate and blood pressure. This type of information is private and highly confidential and hence a secure transmission is of a high demand. However, due to broadcast nature of the wireless medium, the transmission in IoT can be easily detected or eavesdropped on by unauthorized users [1], [2].

Traditional security techniques offer protection against eavesdropping through encryption [3], [4], guaranteeing the integrity of messages over the air. However, it has been shown in the recent years that even the most robust encryption techniques can be defeated by a powerful adversary (e.g., a quantum computer) [5]. Meanwhile, physical-layer security, on the other hand, exploits the dynamic characteristics of the wireless medium to preserve the confidentiality of the transmitted information in wireless networks [6]–[9]. We note that both the conventional encryption and physical layer security techniques cannot provide protection against the detection of a transmission in the first place, which may disclose a user's critical information (e.g., exposing a user's location information). As such, hiding a wireless transmission in the first place is widely required in some IoT applications, which is also explicitly desired by government and military bodies. Against this background, covert communications (also termed low probability of detection communications) are emerging as new and cutting-edge wireless communication security techniques, which aim to enable a wireless transmission between two users while guaranteeing a negligible probability of detecting this transmission at a warden [10]–[15].

In the literature, the fundamental limit of covert communications over additive white Gaussian noise (AWGN) channels has been studied in [10]. It is proved that $\mathcal{O}(\sqrt{n})$ bits of information can be transmitted to a legitimate receiver reliably and covertly in n channel uses as $n \rightarrow \infty$. Following [10], covert communications have been studied in a few scenarios. For example, covert communications can be achieved when the warden has uncertainty about the receiver noise power [16]. In addition to the work of [16], two detail models of the noise uncertainty at the warden and associated approaches to measure the covertness were investigated in [17]. The effect of finite blocklength (i.e., short delay constraints) over AWGN channels on covert communications was examined in [18], which proves that the effective throughput of covert communications is maximized when all available channel uses are utilized. A covert communication system under block fading channels was examined in [19], where transceivers have uncertainty on the related channel state information. Covert communications in the context of relay networks was examined in [20], which shows that a relay can transmit confidential information to the corresponding destination covertly on top of forwarding the source's message.

The aforementioned works in the literature mainly focused on how to hide the wireless transmission action (not the transmitter itself), since some information that can indicate the exist of the transmitter was assumed *a priori* known. For example, in [16]–[20] it is assumed that the instantaneous wireless channels from the transmitter to the warden are known by the warden, which means that the warden knows the existence of the transmitter and is to detect whether a wireless transmission occurs. We note that the ultimate goal of covert communications is to achieve a shadow wireless network [12], in which the transmitter itself should be hidden from the warden. This is due to the fact that the exposure of a user's location information will cause severe negative impact in some applications. For example, when IoT is adopted in battlefields for communication, location information of soldiers or headquarters is extremely confidential, since exposure of this information may lead to fatal attack on the soldiers or headquarters. As such, in this work we aim at an initial step towards this ultimate goal of covert communications by remove some strong assumptions that reveal the existence of the transmitter *a priori*. We adopt the channel inversion power control at the transmitter to achieve covert communications, while

minimizing the *a priori* information on the transmitter in order to achieve the goal of hiding it.

Our main specific contributions are summarized as below.

- Considering practical Rayleigh fading channels in wireless networks, in this work we adopt the channel inversion power control at the transmitter to achieve covert communications, in which the transmitter varies its transmit power as per the channel from itself to the receiver, such that the received power of the covert information signal is a fixed value Q . With channel reciprocity, this power control strategy does not require the transmitter to transmit pilot signals for channel estimation or to feed back the estimated channel to the receiver before covert communications, which may announce the existence of the transmitter before a covert transmission. As such, this power control can potentially aid hiding the transmitter and thus we adopt it in two specific scenarios to achieve covert communications in this work, where its performance is thoroughly examined.
- In the first specific scenario, the possible hiding of the transmitter is achieved by noise uncertainty at the warden, since due to limited resources a transceiver may not be able to learn the wireless environment perfectly. We first analyze the detection performance at the warden, based on which we determine effective covert rate (ECR) that quantifies the amount of information that can be conveyed from the transmitter to the receiver subject to the warden's detection error probability being no less than some specific value. Our examination shows that the increase in the noise uncertainty at the warden and receiver may not continuously improve ECR, since the noise uncertainty at the receiver reduces the transmission reliability from the transmitter to the receiver, although the noise uncertainty at the warden increases its detection error probability.
- Noting that noise uncertainty may not exist when a receiver has sufficient resources (e.g., time) to monitor the wireless communication environment, we consider a full-duplex receiver to aid hiding the transmitter in the second specific scenario, where this receiver deliberately transmits artificial noise (AN) with a random power to confuse the warden on detecting the covert transmission. In this scenario, the detection error probability at the warden is derived in a closed-form expression, based on which the optimal detection threshold is analytically

achieved. The generated AN, although causes self-interference at the receiver, offers the capability of hiding the transmitter. Our analysis shows that the achieved ECR approaches to an analytical upper bound as the transmit power of AN approaches to infinity.

The rest of this paper is organized as follows. Section II details our system model and adopted assumptions. In Section III, we examine the performance of covert communications with noise uncertainty. Section IV presents our analysis on covert communications with the full-duplex receiver. Section V provides numerical results to confirm our analysis and provide useful insights with regard to the impact of some system parameters on covert communications. Section VI draws conclusion remarks.

Notation: Scalar variables are denoted by italic symbols. Vectors are denoted by lower-case boldface symbols. Given a complex number, $|\cdot|$ denotes its modulus.

II. SYSTEM MODEL

A. Considered Communication Scenario

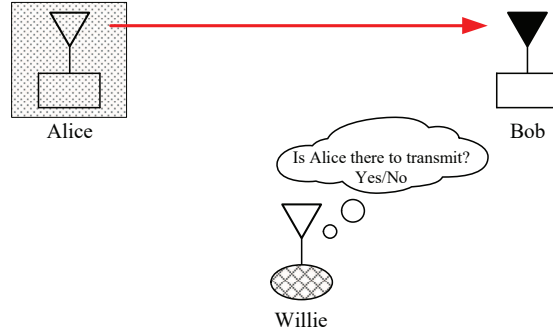


Fig. 1. Covert communications network model.

As shown in Fig. 1, we consider a wireless communication scenario, where Alice (i.e., the transmitter) wants to transmit information covertly to Bob, while trying to hide herself from Willie (i.e., the warden). Meanwhile, Willie is to detect Alice's transmission by observing the wireless environment. We assume the wireless channels within our system model are subject to independent quasi-static Rayleigh fading with equal block length, which means that all the channel coefficients are independent and identically distributed (i.i.d.) circularly symmetric complex Gaussian random variables with zero-mean and unit-variance. We also assume that

each node is equipped with a single antenna. The channel from Bob-to-Alice, Bob-to-Willie, Alice-to-Bob, or Alice-to-Willie, is denoted by h_j and the mean value of $|h_j|^2$ is denoted by λ_j , where the subscript j can be ba, bw, ab, aw , respectively, corresponding to different channels. In this work, from a conservative point of view we assume that λ_j is publicly known, since, for example, Willie can possibly know the location of Bob and the potential area or location (e.g., a room) where Alice can be at.

In order to achieve the ultimate goal of hiding the presence of Alice, in the considered scenario Bob broadcasts pilots periodically in order to enable Alice's estimation of the channel from Bob to Alice (i.e., h_{ba}). Meanwhile, Willie can estimate the channel from Bob to Willie (i.e., h_{bw}), since the pilots transmitted by Bob are publicly known. Considering channel reciprocity, we assume the channel from Alice to Bob is the same as h_{ba} . Since Alice does not transmit any pilots, it is assumed that Willie does not know h_{aw} . To eliminate the requirement that Bob has to know h_{ab} for decoding and avoid the feedback from Alice to Bob, in this work we consider the channel inversion power control at Alice, in which Alice varies its transmit power as per h_{ab} such that $P_a|h_{ab}|^2$ is a fixed value, i.e.,

$$P_a|h_{ab}|^2 = Q, \quad (1)$$

where P_a is the transmit power of Alice. Considering some specific quality of service (QoS) requirements, we consider that the transmission rate from Alice to Bob is fixed and predetermined, which is denoted by R . As such, transmission from Alice to Bob incurs outage when $C_{ab} < R$, where C_{ab} is the channel capacity from Alice to Bob. Then, the transmission outage probability is given by

$$\delta = \mathcal{P}[C_{ab} < R]. \quad (2)$$

As such, in this work we adopt the effective transmission rate as the main performance metric for the communication from Alice to Bob. This effective transmission rate quantifies the rate of the information that is reliably transmitted from Alice to Bob, which is given by

$$R_c = R(1 - \delta). \quad (3)$$

B. Binary Detection at Willie

In the considered communication scenario, Willie is to infer the presence of Alice by detecting the wireless transmission from Alice to Bob. As such, Willie has a binary detection problem, in which Alice does not transmit information to Bob in the null hypothesis \mathcal{H}_0 but it does in the alternative hypothesis \mathcal{H}_1 . The ultimate goal for Willie is to detect whether his observation comes from \mathcal{H}_0 or \mathcal{H}_1 by applying some specific decision rule. The detection performance of Willie is normally measured by the detection error probability, which is defined as

$$\xi \triangleq \alpha + \beta, \quad (4)$$

where $\alpha = \mathcal{P}(\mathcal{D}_1|\mathcal{H}_0)$ is the false alarm rate and $\beta = \mathcal{P}(\mathcal{D}_0|\mathcal{H}_1)$ is the miss detection rate, while \mathcal{D}_1 and \mathcal{D}_0 are the binary decisions that infer whether Alice transmits information to Bob or not, respectively. From a conservative point of view, in this work we consider the worst-case scenario for Alice and Bob, where Willie has the ability to develop the optimal detection strategy with a sufficient test statistic and the optimal detection threshold on it. The optimal detection strategy at Willie can achieve the minimum detection error probability. As such, the covert communication constraint considered in this work is that the minimum detection error probability at Willie should be no less than $1 - \epsilon$, where $\epsilon \in [0, 1]$ is a predetermined value to specify the covert communication constraint [17], [19].

III. CHANNEL INVERSION POWER CONTROL WITH NOISE UNCERTAINTY

Receiver noise in wireless communications is caused by various independent sources, including but not limited to thermal noise at the receiver and the interference due to nearby emissions [21]. In most works of literature in wireless communications, it is assumed that the receiver noise is Gaussian due to the Central Limit Theorem (CLT) and the noise power is known given the ideal assumption that the receiver has sufficient resource (e.g., time) to learn the statistic information on the receiver noise before the communication from the transmitter to the receiver. However, in practice a receiver may move to a new scenario and cannot learn the full statistical information on the receiver noise [17], [22], [23]. In addition, temperature change, environmental noise change, and calibration error may also cause noise uncertainty at a receiver. Therefore, considering noise

uncertainty is practical and necessary for the detection problem at Willie. As such, in this section we consider the noise uncertainty at both Bob and Willie, since this uncertainty leads to a non-zero detection error probability at Willie such that enables the covert transmission from Alice to Bob.

A. Noise Uncertainty Model

Following [17], [22], [23], in this work we adopt the bounded uncertainty model, in which the true received noise power σ_k^2 lies in a finite range around the nominal noise power $\hat{\sigma}_k^2$, where the subscript k can be b or w , corresponding to the noise uncertainty at Bob or Willie, respectively. More specifically, we assume that $\sigma_{k,\text{dB}}^2$ (i.e., σ_k^2 in dB domain) is uniformly distributed within $[\hat{\sigma}_{k,\text{dB}}^2 - \rho_{k,\text{dB}}, \hat{\sigma}_{k,\text{dB}}^2 + \rho_{k,\text{dB}}]$, where $\rho_{k,\text{dB}} = 10 \log_{10}(\rho_k)$ is the parameter that quantifies the size of the uncertainty [17], [23]. Then, the probability density function (pdf) of σ_k for the adopted bounded uncertainty model is given by

$$f_{\sigma_k^2}(x) = \begin{cases} \frac{1}{2 \ln(\rho_k)x}, & \text{if } \frac{\hat{\sigma}_k^2}{\rho_k} \leq x \leq \rho_k \hat{\sigma}_k^2, \\ 0, & \text{otherwise.} \end{cases} \quad (5)$$

B. Transmission from Alice to Bob

In this subsection, we first detail the transmission from Alice to Bob and then derive the associated transmission outage probability.

When Alice transmits, the signal received at Bob is given by

$$\mathbf{y}_b[i] = \sqrt{P_a} h_{ab} \mathbf{x}_a[i] + \mathbf{n}_b[i], \quad (6)$$

where \mathbf{x}_a is the signal transmitted by Alice satisfying $\mathbb{E}[\mathbf{x}_a[i] \mathbf{x}_a^\dagger[i]] = 1$, $i = 1, 2, \dots, n$ is the index of each channel use, and $\mathbf{n}_b[i]$ is the AWGN at Bob with σ_b^2 as its variance, i.e., $\mathbf{n}_b[i] \sim \mathcal{CN}(0, \sigma_b^2)$. Following (1) and (6), the signal to noise ratio (SNR) at Bob is given by

$$\gamma_b = \frac{P_a |h_{ab}|^2}{\sigma_b^2} = \frac{Q}{\sigma_b^2}. \quad (7)$$

Considering the noise uncertainty at Bob, the transmission from Alice to Bob may occur outage and we derive the transmission outage probability in the following lemma.

Proposition 1: The transmission outage probability from Alice to Bob is given by

$$\delta = \begin{cases} 1, & \text{if } \frac{Q}{2^R - 1} < \frac{\hat{\sigma}_b^2}{\rho_b}, \\ \frac{1}{2 \ln(\rho_b)} \ln \left(\frac{(2^R - 1) \hat{\sigma}_b^2 \rho_b}{Q} \right), & \text{if } \frac{\hat{\sigma}_b^2}{\rho_b} \leq \frac{Q}{2^R - 1} \leq \rho_b \hat{\sigma}_b^2, \\ 0, & \text{if } \frac{Q}{2^R - 1} > \rho_b \hat{\sigma}_b^2. \end{cases} \quad (8)$$

Proof: Based on the definition of the transmission outage probability given in (2), the bounded noise uncertainty model given in (5), and (7), we have

$$\begin{aligned} \delta &= \mathcal{P} \{ \log_2(1 + \gamma_b) \leq R \} \\ &= \mathcal{P} \left\{ \frac{Q}{2^R - 1} \leq \sigma_b^2 \right\} \\ &= \begin{cases} 1, & \text{if } \frac{Q}{2^R - 1} < \frac{\hat{\sigma}_b^2}{\rho_b}, \\ \int_{\frac{Q}{2^R - 1}}^{\rho_b \hat{\sigma}_b^2} \frac{1}{2 \ln(\rho_b) x} dx, & \text{if } \frac{\hat{\sigma}_b^2}{\rho_b} \leq \frac{Q}{2^R - 1} \leq \rho_b \hat{\sigma}_b^2, \\ 0, & \text{if } \frac{Q}{2^R - 1} > \rho_b \hat{\sigma}_b^2. \end{cases} \quad (9) \end{aligned}$$

Then, solving the integral in the above equation leads to the desired result given in (8). \blacksquare

We next examine the impact of the noise uncertainty on the detection performance at Willie in the following subsection.

C. Detection Performance at Willie

In this subsection, we first analyze the detection performance of Willie in terms of deriving its false alarm and miss detection rates, based on which we determine the optimal threshold that minimizes the detection error probability at Willie.

In the considered system model, Willie will detect whether Alice transmits the covert message \mathbf{x}_c to Bob based on his observations. Alice does not transmit \mathbf{x}_c in the null hypothesis \mathcal{H}_0 , while it does in the alternative hypothesis \mathcal{H}_1 . Then, the received signal at Willie is given by

$$\mathbf{y}_w[i] = \begin{cases} \mathbf{n}_w[i], & \mathcal{H}_0, \\ \sqrt{P_a} h_{aw} \mathbf{x}_a[i] + \mathbf{n}_w[i], & \mathcal{H}_1. \end{cases} \quad (10)$$

Considering that each element in \mathbf{x}_a and \mathbf{n}_w are i.i.d, as per (10) the likelihood functions of the observations \mathbf{y}_w under \mathcal{H}_0 and \mathcal{H}_1 are, respectively, given by

$$\begin{aligned} f(\mathbf{y}_w|\mathcal{H}_0) &= \prod_{i=1}^n f(y_w[i]|\mathcal{H}_0) \\ &= \frac{1}{(2\pi\sigma_w^2)^{\frac{n}{2}}} \exp\left\{-\frac{1}{2\sigma_w^2} \sum_{i=1}^n |y_w[i]|^2\right\}, \end{aligned} \quad (11)$$

$$\begin{aligned} f(\mathbf{y}_w|\mathcal{H}_1) &= \prod_{i=1}^n f(y_w[i]|\mathcal{H}_1) \\ &= \frac{1}{(2\pi(P_a|h_{aw}|^2 + \sigma_w^2))^{\frac{n}{2}}} \exp\left\{-\frac{1}{2(P_a|h_{aw}|^2 + \sigma_w^2)} \sum_{i=1}^n |y_w[i]|^2\right\}. \end{aligned} \quad (12)$$

Following (11) and (12), based on the Fisher-Neyman factorization theorem [24], we note that the term $T(n) = \sum_{i=1}^n |y_w[i]|^2$ is a sufficient test statistic at Willie. In this work, we consider the infinite blocklength, i.e., $n \rightarrow \infty$, where we have

$$T \triangleq \lim_{n \rightarrow \infty} \frac{1}{n} T(n) = \begin{cases} \sigma_w^2, & \mathcal{H}_0, \\ P_a|h_{aw}|^2 + \sigma_w^2, & \mathcal{H}_1. \end{cases} \quad (13)$$

Then, the decision rule in the adopted detector at Willie can be written as

$$T \underset{\mathcal{D}_0}{\overset{\mathcal{D}_1}{\geq}} \tau, \quad (14)$$

where τ is the threshold for T , which will be optimized later in order to minimize the detection error probability. Following (14), we derive the false alarm and miss detection rates at Willie for an arbitrary threshold τ in the following theorem, based on which we will tackle the optimization of τ in Proposition 2.

Theorem 1: The false alarm and miss detection rates at Willie for an arbitrary detection threshold τ are, respectively, derived as

$$\alpha = \begin{cases} 1, & \tau < \frac{\hat{\sigma}_w^2}{\rho_w}, \\ \frac{\ln(\rho_w \hat{\sigma}_w^2) - \ln(\tau)}{2 \ln(\rho_w)}, & \frac{\hat{\sigma}_w^2}{\rho_w} \leq \tau \leq \rho_w \hat{\sigma}_w^2, \\ 0, & \tau > \rho_w \hat{\sigma}_w^2, \end{cases} \quad (15)$$

$$\beta = \begin{cases} 0, & \tau < \frac{\hat{\sigma}_w^2}{\rho_w}, \\ \frac{\tau \lambda_{ab} \ln\left(\frac{\rho_w \tau}{\hat{\sigma}_w^2}\right) + Q \lambda_{aw} \ln\left(\frac{Q \lambda_{aw}}{Q \lambda_{aw} + \lambda_{ab} \left(\tau - \frac{\hat{\sigma}_w^2}{\rho_w}\right)}\right)}{2 \ln(\rho_w)(Q \lambda_{aw} + \tau \lambda_{ab})}, & \frac{\hat{\sigma}_w^2}{\rho_w} \leq \tau \leq \rho_w \hat{\sigma}_w^2, \\ \frac{2 \tau \lambda_{ab} \ln(\rho_w) + Q \lambda_{aw} \ln\left(\frac{Q \lambda_{aw} + \lambda_{ab} \left(\tau - \rho_w \hat{\sigma}_w^2\right)}{Q \lambda_{aw} + \lambda_{ab} \left(\tau - \frac{\hat{\sigma}_w^2}{\rho_w}\right)}\right)}{2 \ln(\rho_w)(Q \lambda_{aw} + \tau \lambda_{ab})}, & \tau > \rho_w \hat{\sigma}_w^2. \end{cases} \quad (16)$$

Proof: Following (5), (13), and (14), the false alarm rate is given by

$$\begin{aligned} \alpha &= \mathcal{P} [\sigma_w^2 > \tau] \\ &= \begin{cases} 0, & \tau < \frac{\hat{\sigma}_w^2}{\rho_w}, \\ \int_{\tau}^{\rho_w \hat{\sigma}_w^2} f_{\sigma_w^2}(x) dx & \frac{\hat{\sigma}_w^2}{\rho_w} \leq \tau \leq \rho_w \hat{\sigma}_w^2, \\ 1, & \tau > \rho_w \hat{\sigma}_w^2, \end{cases} \\ &= \begin{cases} 0, & \tau < \frac{\hat{\sigma}_w^2}{\rho_w}, \\ \int_{\tau}^{\rho_w \hat{\sigma}_w^2} \frac{1}{2 \ln(\rho_w) x} dx, & \frac{\hat{\sigma}_w^2}{\rho_w} \leq \tau \leq \rho_w \hat{\sigma}_w^2, \\ 1, & \tau > \rho_w \hat{\sigma}_w^2. \end{cases} \end{aligned} \quad (17)$$

Then, solving the integral in (17) leads to the desired result in (15).

Likewise, the miss detection rate is given by

$$\begin{aligned} \beta &= \mathcal{P} [P_a | h_{aw}|^2 + \sigma_w^2 < \tau] \\ &= \mathcal{P} \left[\frac{Q |h_{aw}|^2}{|h_{ab}|^2} + \sigma_w^2 < \tau \right] \\ &= \begin{cases} 0, & \tau < \frac{\hat{\sigma}_w^2}{\rho_w}, \\ \int_{\frac{\hat{\sigma}_w^2}{\rho_w}}^{\tau} \int_0^{+\infty} \int_0^{\frac{(\tau-z)y}{Q}} f_{|h_{aw}|^2}(x) f_{|h_{ab}|^2}(y) f_{\sigma_w^2}(z) dx dy dz, & \frac{\hat{\sigma}_w^2}{\rho_w} \leq \tau \leq \rho_w \hat{\sigma}_w^2, \\ \int_{\frac{\hat{\sigma}_w^2}{\rho_w}}^{\rho_w \hat{\sigma}_w^2} \int_0^{+\infty} \int_0^{\frac{(\tau-z)y}{Q}} f_{|h_{aw}|^2}(x) f_{|h_{ab}|^2}(y) f_{\sigma_w^2}(z) dx dy dz, & \tau > \rho_w \hat{\sigma}_w^2, \end{cases} \\ &= \begin{cases} 0, & \tau < \frac{\hat{\sigma}_w^2}{\rho_w}, \\ \int_{\frac{\hat{\sigma}_w^2}{\rho_w}}^{\tau} \int_0^{+\infty} \int_0^{\frac{(\tau-z)y}{Q}} \frac{\exp\left\{-\left(\frac{x}{\lambda_{aw}} + \frac{y}{\lambda_{ab}}\right)\right\}}{2 \lambda_{aw} \lambda_{ab} \ln(\rho_w) z} dx dy dz, & \frac{\hat{\sigma}_w^2}{\rho_w} \leq \tau \leq \rho_w \hat{\sigma}_w^2, \\ \int_{\frac{\hat{\sigma}_w^2}{\rho_w}}^{\rho_w \hat{\sigma}_w^2} \int_0^{+\infty} \int_0^{\frac{(\tau-z)y}{Q}} \frac{\exp\left\{-\left(\frac{x}{\lambda_{aw}} + \frac{y}{\lambda_{ab}}\right)\right\}}{2 \lambda_{aw} \lambda_{ab} \ln(\rho_w) z} dx dy dz, & \tau > \rho_w \hat{\sigma}_w^2, \end{cases} \\ &= \begin{cases} 0, & \tau < \frac{\hat{\sigma}_w^2}{\rho_w}, \\ \int_{\frac{\hat{\sigma}_w^2}{\rho_w}}^{\tau} \int_0^{+\infty} \frac{(1 - \exp(-\frac{(\tau-z)y}{Q})) \exp\left(-\frac{y}{\lambda_{ab}}\right)}{2 \lambda_{aw} \lambda_{ab} \ln(\rho_w) z} dy dz, & \frac{\hat{\sigma}_w^2}{\rho_w} \leq \tau \leq \rho_w \hat{\sigma}_w^2, \\ \int_{\frac{\hat{\sigma}_w^2}{\rho_w}}^{\rho_w \hat{\sigma}_w^2} \int_0^{+\infty} \frac{(1 - \exp(-\frac{(\tau-z)y}{Q})) \exp\left(-\frac{y}{\lambda_{ab}}\right)}{2 \lambda_{aw} \lambda_{ab} \ln(\rho_w) z} dy dz, & \tau > \rho_w \hat{\sigma}_w^2, \end{cases} \end{aligned}$$

$$= \begin{cases} 0, & \tau < \frac{\hat{\sigma}_w^2}{\rho_w}, \\ \int_{\frac{\hat{\sigma}_w^2}{\rho_w}}^{\tau} \frac{(\tau-z)\lambda_{ab}}{2 \ln(\rho_w)z((\tau-z)\lambda_{ab}+Q\lambda_{aw})} dz, & \frac{\hat{\sigma}_w^2}{\rho_w} \leq \tau \leq \rho_w \hat{\sigma}_w^2, \\ \int_{\frac{\hat{\sigma}_w^2}{\rho_w}}^{\rho_w \hat{\sigma}_w^2} \frac{(\tau-z)\lambda_{ab}}{2 \ln(\rho_w)z((\tau-z)\lambda_{ab}+Q\lambda_{aw})} dz, & \tau > \rho_w \hat{\sigma}_w^2. \end{cases} \quad (18)$$

Following (18), we achieve the desired result in (16) after some algebra manipulations. \blacksquare

Following Theorem 1, we next tackle the optimal threshold that minimizes the detection error probability in the following proposition.

Proposition 2: The optimal threshold that minimizes ξ at Willie with noise uncertainty can be obtained through

$$\tau^* = \underset{\hat{\sigma}_w^2/\rho_w \leq \tau \leq \rho_w \hat{\sigma}_w^2}{\operatorname{argmin}} \frac{\tau \lambda_{ab} \ln\left(\frac{\rho_w \tau}{\hat{\sigma}_w^2}\right) + Q \lambda_{aw} \ln\left(\frac{Q \lambda_{aw}}{Q \lambda_{aw} + \lambda_{ab} \left(\tau - \frac{\hat{\sigma}_w^2}{\rho_w}\right)}\right)}{2 \ln(\rho_w)(Q \lambda_{aw} + \tau \lambda_{ab})}. \quad (19)$$

Proof: Following (15) and (16), the detection error probability at Willie with noise uncertainty is given by

$$\xi = \begin{cases} 1, & \tau < \frac{\hat{\sigma}_w^2}{\rho_w}, \\ \frac{2 \ln(\rho_w) \tau \lambda_{ab} + Q \lambda_{aw} \ln\left(\frac{\rho_w \hat{\sigma}_w^2 Q \lambda_{aw}}{\tau (Q \lambda_{aw} + \lambda_{ab} \left(\tau - \frac{\hat{\sigma}_w^2}{\rho_w}\right))}\right)}{2 \ln(\rho_w)(Q \lambda_{aw} + \tau \lambda_{ab})}, & \frac{\hat{\sigma}_w^2}{\rho_w} \leq \tau \leq \rho_w \hat{\sigma}_w^2, \\ \frac{2 \ln(\rho_w) \tau \lambda_{ab} + Q \lambda_{aw} \ln\left(\frac{Q \lambda_{aw} + \lambda_{ab} \left(\tau - \rho_w \hat{\sigma}_w^2\right)}{Q \lambda_{aw} + \lambda_{ab} \left(\tau - \frac{\hat{\sigma}_w^2}{\rho_w}\right)}\right)}{2 \ln(\rho_w)(Q \lambda_{aw} + \tau \lambda_{ab})}, & \tau > \rho_w \hat{\sigma}_w^2. \end{cases} \quad (20)$$

We first note that $\xi = 1$ is the worst case for Willie and thus Willie does not set $\tau < \hat{\sigma}_w^2/\rho_w$.

For $\tau > \rho_w \hat{\sigma}_w^2$, we derive the first derivative of ξ with respect to τ as

$$\begin{aligned} \frac{\partial \xi}{\partial \tau} &= \frac{Q \lambda_{aw}}{2 \ln(\rho_w)(Q \lambda_{aw} + \tau \lambda_{ab})^2} \left\{ 2 \ln(\rho_w) + (Q \lambda_{aw} + \tau \lambda_{ab}) \times \right. \\ &\quad \left. \left(\frac{1}{\lambda_{ab}(\tau - \rho_w \hat{\sigma}_w^2) + Q \lambda_{aw}} - \frac{1}{\lambda_{ab}(\tau - \frac{\hat{\sigma}_w^2}{\rho_w}) + Q \lambda_{aw}} \right) - \ln\left(\frac{\lambda_{ab}(\tau - \rho_w \hat{\sigma}_w^2) + Q \lambda_{aw}}{\lambda_{ab}(\tau - \frac{\hat{\sigma}_w^2}{\rho_w}) + Q \lambda_{aw}}\right) \right\}, \\ &= \frac{Q \lambda_{aw}}{2 \ln(\rho_w)(Q \lambda_{aw} + \tau \lambda_{ab})^2} \{2 \ln(\rho_w) + g(\tau)\}, \end{aligned} \quad (21)$$

where

$$\begin{aligned} g(\tau) &= (Q \lambda_{aw} + \tau \lambda_{ab}) \left(\frac{1}{\lambda_{ab}(\tau - \rho_w \hat{\sigma}_w^2) + Q \lambda_{aw}} - \frac{1}{\lambda_{ab}(\tau - \frac{\hat{\sigma}_w^2}{\rho_w}) + Q \lambda_{aw}} \right) \\ &\quad - \ln\left(\frac{\lambda_{ab}(\tau - \rho_w \hat{\sigma}_w^2) + Q \lambda_{aw}}{\lambda_{ab}(\tau - \frac{\hat{\sigma}_w^2}{\rho_w}) + Q \lambda_{aw}}\right). \end{aligned} \quad (22)$$

In order to check the sign of (21), we derive the first derivative of $g(\tau)$ with respect to τ as

$$\frac{\partial g(\tau)}{\partial \tau} = -\lambda_{ab}(Q\lambda_{aw} + \tau\lambda_{ab}) \times \left(\frac{1}{(\lambda_{ab}(\tau - \rho_w \hat{\sigma}_w^2) + Q\lambda_{aw})^2} - \frac{1}{(\lambda_{ab}(\tau - \frac{\hat{\sigma}_w^2}{\rho_w}) + Q\lambda_{aw})^2} \right). \quad (23)$$

Noting the fact that $\rho_w > 1$, as per (23) we can see that $\frac{\partial g(\tau)}{\partial \tau} < 0$ for $\tau > \rho_w \hat{\sigma}_w^2$. Following the definition of $g(\tau)$ given in (22), we also note that $\lim_{\tau \rightarrow \infty} g(\tau) = 0$. As such, we have $g(\tau) > 0$. Again, noting $\rho_w > 1$ and following (21), we can conclude that $\partial \xi / \partial \tau > 0$, which indicates that ξ monotonically increases with τ for $\tau > \rho_w \hat{\sigma}_w^2$. Considering that ξ is a continuous function of τ , we can conclude that the optimal detection threshold τ^* should satisfy $\hat{\sigma}_w^2 / \rho_w \leq \tau^* \leq \rho_w \hat{\sigma}_w^2$, which completes the proof of Proposition 2. ■

Substituting τ^* into (20), we can obtain the minimum detection error probability ξ^* at Willie with noise uncertainty.

D. Optimization of Effective Covert Rate

The optimal value of Q that maximizes R_c subject to the covert constraint $\xi^* \geq 1 - \epsilon$ can be obtained through

$$Q^* = \underset{Q}{\operatorname{argmax}} R_c \quad (24)$$

$$\text{s.t. } \xi^* \geq 1 - \epsilon.$$

Following Proposition 2, we note that the optimization problem (24) is of one dimension, which can be solved by some efficient numerical search methods. The maximum value of R_c is then achieved by substituting Q^* into R_c , which is denoted by R_c^* .

IV. CHANNEL INVERSION POWER CONTROL WITH A FULL-DUPLEX RECEIVER

In this section, we examine the possibility and performance of covert communications by utilizing AN generated by the full-duplex Bob (i.e., the receiver), since this AN can lead to a certain amount of uncertainty at Willie when the noise uncertainty is not present (e.g., when Willie has sufficient resource to learn the wireless environment). Relative to utilizing the noise

uncertainty, generating AN by the full-duplex Bob enables varying the presence and amount of uncertainty at Willie on demand, which leads to that the covert communication between Alice and Bob is fully under the control of Alice and Bob.

Following [25], in this section we consider a specific covert wireless communication scenario, where Bob (i.e., the receiver) operates in full-duplex mode and Alice (i.e., the transmitter) wants to transmit covertly to Bob with the aid of AN generated by Bob, while Willie (i.e., the warden) tries to detect this covert transmission. Besides the single receiving antenna, Bob uses an additional antenna for transmission of AN in order to deliberately confuse Willie. We note that our current analysis in this section is significantly different from [25], although the considered scenario is similar. This is due to the following two facts. The first fact is that in [25] it is assumed that Willie knows the channel from Alice to Willie (i.e., h_{aw}), while in this section we assume that h_{aw} is unknown to Willie (since Alice did not transmit any signal before the covert transmission). The second fact is that in this work we adopt the channel inversion power control at Alice, while in [25] a fixed power is adopted at Alice.

A. Transmission from Alice to Bob

In this subsection, we detail the transmission from Alice to the full-duplex Bob and derive the associated transmission outage probability.

When Alice transmits the covert information, the signal received at the full-duplex Bob is given by

$$\mathbf{y}_b[i] = \sqrt{P_a}h_{ab}\mathbf{x}_a[i] + \sqrt{\phi P_b}h_{bb}\mathbf{v}_b[i] + \mathbf{n}_b[i], \quad (25)$$

where \mathbf{v}_b is the AN signal transmitted by Bob satisfying $\mathbb{E}[\mathbf{v}_b[i]\mathbf{v}_b^\dagger[i]] = 1$, h_{bb} denotes the self-interference channel at Bob (i.e., the channel between Bob's transmitting antenna and Bob's receiving antenna), and P_b is Bob's transmit power of the AN signal. We assume that the mean value of $|h_{bb}|^2$ is λ_{bb} . In (25), we recall that \mathbf{x}_a is the signal transmitted by Alice satisfying $\mathbb{E}[\mathbf{x}_a[i]\mathbf{x}_a^\dagger[i]] = 1$, $i = 1, 2, \dots, n$ is the index of each channel use, and $\mathbf{n}_b[i]$ is the AWGN at Bob with σ_b^2 as its variance, i.e., $\mathbf{n}_b[i] \sim \mathcal{CN}(0, \sigma_b^2)$. Since the AN signal is known to Bob, the residual noise can be rebuilt and eliminated by self-interference cancellation techniques [26]. In

this work, we assume that the self-interference cannot be totally cancelled and we denote the self-interference cancellation coefficient by ϕ in (25). We note that $0 < \phi \leq 1$ corresponds to different self-interference cancellation levels [27]. In order to create uncertainty at Willie, in this work we assume that P_b changes from slot to slot and follows a continuous uniform distribution over the interval $[0, P_b^{\max}]$ with pdf given by

$$f_{P_b}(x) = \begin{cases} \frac{1}{P_b^{\max}} & \text{if } 0 \leq x \leq P_b^{\max}, \\ 0, & \text{otherwise.} \end{cases} \quad (26)$$

Since Willie possesses the knowledge of h_{aw} and h_{bw} in the slot under consideration, for a constant transmit power at Bob, it is straightforward for him to detect the covert transmission when the additional power (on top of his receiver noise power) is received. The purpose of introducing randomness in Bob's transmit power is to create uncertainty in Willie's received power, such that Willie is unsure whether an increase in his received power is due to Alice's transmission or simply due to a variation in Bob's transmit power of the AN signal. We note that we consider the uniform distribution as an initial example and other distributions will be explored in our future works.

Following (25), the signal to interference plus noise ratio (SINR) at Bob used to decode \mathbf{x}_a is given by

$$\gamma_b = \frac{P_a |h_{ab}|^2}{\phi P_b |h_{bb}|^2 + \sigma_b^2} = \frac{Q}{\phi P_b |h_{bb}|^2 + \sigma_b^2}, \quad (27)$$

since Alice varies its transmit power as per h_{ab} such that $P_a |h_{ab}|^2 = Q$. Due to the randomness in $|h_{bb}|^2$ and P_b that is unknown to Bob, the transmission from Alice to Bob will incur outage when $C_{ab} < R$, where $C_{ab} = \log_2(1 + \gamma_b)$ is the channel capacity from Alice to Bob and R is the fixed transmission rate from Alice to Bob. We note that γ_b cannot be larger than Q/σ_b^2 , which is achieved when $\phi = 0$ (i.e., when the self-interference can be fully cancelled). As such, in order to guarantee the transmission outage probability being less than one, we to have to ensure $R < \log_2(1 + Q/\sigma_b^2)$, which is assumed to be true in this section. We next derive the transmission outage probability from Alice to Bob in the following proposition.

Proposition 3: The transmission outage probability from Alice to the full-duplex Bob is derived

as

$$\delta = e^{-\eta} - \eta \text{Ei}(-\eta), \quad (28)$$

where

$$\eta = \frac{Q - (2^R - 1)\sigma_b^2}{(2^R - 1)\lambda_{bb}\phi P_b^{\max}}, \quad (29)$$

and the exponential integral function $\text{Ei}(\cdot)$ is given by

$$\text{Ei}(x) = - \int_{-x}^{\infty} \frac{e^{-\theta}}{\theta} d\theta, \quad [x < 0]. \quad (30)$$

Proof: Based on the definition of the transmission outage probability given in (2), we have

$$\begin{aligned} \delta &= \mathcal{P} \{ \log_2(1 + \gamma_b) \leq R \} \\ &= \mathcal{P} \left\{ \frac{Q}{\phi P_b |h_{bb}|^2 + \sigma_b^2} \leq 2^R - 1 \right\} \\ &= \int_0^{P_b^{\max}} \int_{\frac{Q - (2^R - 1)\sigma_b^2}{(2^R - 1)\phi y}}^{+\infty} f_{|h_{bb}|^2}(x) f_{P_b}(y) dx dy \\ &= \int_0^{P_b^{\max}} \int_{\frac{Q - (2^R - 1)\sigma_b^2}{(2^R - 1)\phi y}}^{+\infty} \frac{\exp\left(-\frac{x}{\lambda_{bb}}\right)}{\lambda_{bb} P_b^{\max}} dx dy \\ &= \frac{1}{P_b^{\max}} \int_0^{P_b^{\max}} \exp\left\{ -\frac{Q - (2^R - 1)\sigma_b^2}{(2^R - 1)\lambda_{bb}\phi y} \right\} dy \\ &= \exp\left(-\frac{Q - (2^R - 1)\sigma_b^2}{(2^R - 1)\lambda_{ab}\phi P_b^{\max}} \right) \\ &\quad - \frac{Q - (2^R - 1)\sigma_b^2}{(2^R - 1)\lambda_{ab}\phi P_b^{\max}} \text{Ei}\left(-\frac{Q - (2^R - 1)\sigma_b^2}{(2^R - 1)\lambda_{ab}\phi P_b^{\max}} \right). \end{aligned} \quad (31)$$

Following (31), we achieve the desired result in (28) after some algebra manipulations. \blacksquare

Following Proposition 3, we determine some properties of the transmission outage probability in the following corollary.

Corollary 1: The transmission outage probability δ is a monotonically decreasing function of η , which leads to the fact that δ monotonically decreases with Q but increases with P_b^{\max} .

Proof: Following (28) and (30), the expression of transmission outage probability δ can be rewritten as

$$\begin{aligned}\delta &= e^{-\eta} - \eta \int_{\eta}^{\infty} \frac{e^{-\theta}}{\theta} d\theta \\ &= e^{-\eta} - \eta \left(\int_0^{\infty} \frac{e^{-\theta}}{\theta} d\theta - \int_0^{\eta} \frac{e^{-\theta}}{\theta} d\theta \right).\end{aligned}\quad (32)$$

In order to determine the monotonicity of δ with respect to τ , we derive its first derivative as

$$\begin{aligned}\frac{\partial \delta}{\partial \eta} &= -e^{-\eta} - \left(\int_0^{\infty} \frac{e^{-\theta}}{\theta} d\theta - \int_0^{\eta} \frac{e^{-\theta}}{\theta} d\theta \right) - \eta \left(-\frac{e^{-\eta}}{\eta} \right) \\ &= - \int_{\eta}^{\infty} \frac{e^{-\theta}}{\theta} d\theta = \text{Ei}(-\eta).\end{aligned}\quad (33)$$

We note that $\eta \geq 0$ as per its definition given in (29) and thus we have $\partial \delta / \partial \eta \leq 0$ due to $\text{Ei}(-\eta) < 0$, which indicates that δ monotonically decreases with η . Again, as per the definition of η in (29), we can see that η is a monotonically increasing function of Q but a monotonically decreasing function of P_b^{\max} , which completes the proof of Corollary 1. ■

B. Detection Performance at Willie

In this subsection, we examine the detection performance at Willie in the considered scenario with the full-duplex Bob. Specifically, we derive the false alarm and miss detection rates at Willie, based on which we derive the optimal detection threshold that minimizes the detection error probability.

We focus on one communication slot, where Willie has to decide whether Alice transmitted to Bob, or not. Thus Willie faces a binary hypothesis testing problem. The composite received signal model at Willie is given by

$$\mathbf{y}_w[i] = \begin{cases} \sqrt{P_b} h_{bw} \mathbf{v}_b[i] + \mathbf{n}_w[i], & \mathcal{H}_0, \\ \sqrt{P_a} h_{aw} \mathbf{x}_a[i] + \sqrt{P_b} h_{bw} \mathbf{v}_b[i] + \mathbf{n}_w[i], & \mathcal{H}_1. \end{cases}\quad (34)$$

We recall that the value of P_b in the given slot is unknown to Willie, the likelihood functions of the observations \mathbf{y}_w under \mathcal{H}_0 and \mathcal{H}_1 are, respectively, given by

$$\begin{aligned} f(\mathbf{y}_w | \mathcal{H}_0) &= \prod_{i=1}^n f(\mathbf{y}_w[i] | \mathcal{H}_0) \\ &= \frac{1}{(2\pi (P_a |h_{aw}|^2 + \sigma_w^2))^{\frac{n}{2}}} \exp \left\{ -\frac{1}{2 (P_a |h_{aw}|^2 + \sigma_w^2)} \sum_{i=1}^n |\mathbf{y}_w[i]|^2 \right\}, \end{aligned} \quad (35)$$

$$\begin{aligned} f(\mathbf{y}_w | \mathcal{H}_1) &= \prod_{i=1}^n f(\mathbf{y}_w[i] | \mathcal{H}_1) \\ &= \frac{1}{(2\pi (P_a |h_{aw}|^2 + P_b |h_{bw}|^2 + \sigma_w^2))^{\frac{n}{2}}} \exp \left\{ -\frac{1}{2 (P_a |h_{aw}|^2 + P_b |h_{bw}|^2 + \sigma_w^2)} \sum_{i=1}^n |\mathbf{y}_w[i]|^2 \right\}. \end{aligned} \quad (36)$$

Following (35) and (36), based on the Fisher-Neyman factorization theorem [24], we again note that the term $T(n) = \sum_{i=1}^n |\mathbf{y}_s[i]|^2$ is a sufficient test statistic for the detector at Willie.

Considering the infinite blocklength, i.e., $n \rightarrow \infty$, we have

$$T \triangleq \lim_{n \rightarrow \infty} \frac{1}{n} T(n) = \begin{cases} P_b |h_{bw}|^2 + \sigma_w^2, & \mathcal{H}_0, \\ P_a |h_{aw}|^2 + P_b |h_{bw}|^2 + \sigma_w^2, & \mathcal{H}_1. \end{cases} \quad (37)$$

Then, the decision rule embedded in the detector at Willie is given by

$$T \underset{\mathcal{D}_0}{\overset{\mathcal{D}_1}{\geq}} \tau, \quad (38)$$

where τ is the detection threshold for T , which will be optimally determined in order to minimize the detection error probability. Following the decision rule given in (38), we derive the false alarm and miss detection rates at Willie in the considered scenario with the full-duplex Bob in the following theorem.

Theorem 2: The false alarm and miss detection rates at Willie are derived, respectively, as

$$\alpha = \begin{cases} 1, & \tau < \sigma_w^2, \\ 1 - \frac{\tau - \sigma_w^2}{P_b^{\max} |h_{bw}|^2}, & \sigma_w^2 \leq \tau \leq \nu, \\ 0, & \tau > \nu, \end{cases} \quad (39)$$

$$\beta = \begin{cases} 0, & \tau < \sigma_w^2, \\ \frac{1}{P_b^{\max} |h_{bw}|^2} \left(\tau - \sigma_w^2 - \frac{Q \lambda_{aw}}{\lambda_{ab}} \ln \left(1 + \frac{(\tau - \sigma_w^2) \lambda_{ab}}{Q \lambda_{aw}} \right) \right), & \sigma_w^2 \leq \tau \leq \nu, \\ 1 - \frac{Q \lambda_{aw}}{P_b^{\max} |h_{bw}|^2 \lambda_{ab}} \ln \left(1 + \frac{P_b^{\max} |h_{bw}|^2}{\tau + Q \lambda_{aw} / \lambda_{ab} - \nu} \right), & \tau > \nu, \end{cases} \quad (40)$$

where

$$\nu \triangleq P_b^{\max} |h_{bw}|^2 + \sigma_w^2. \quad (41)$$

Proof: Following (37) and (38), the false alarm rate is given by

$$\begin{aligned} \alpha &= \mathcal{P} [P_b |h_{bw}|^2 + \sigma_w^2 > \tau] \\ &= \begin{cases} 1, & \tau < \sigma_w^2, \\ \int_{\frac{\tau - \sigma_w^2}{|h_{bw}|^2}}^{P_b^{\max}} f_{P_b}(x) dx, & \sigma_w^2 \leq \tau \leq \nu, \\ 0, & \tau > \nu, \end{cases} \\ &= \begin{cases} 1, & \tau < \sigma_w^2, \\ \int_{\frac{\tau - \sigma_w^2}{|h_{bw}|^2}}^{P_b^{\max}} \frac{1}{P_b^{\max}} dx, & \sigma_w^2 \leq \tau \leq \nu, \\ 0, & \tau > \nu. \end{cases} \end{aligned} \quad (42)$$

Then, solving the integral in (42) leads to the desired result in (39).

As per (37) and (38), the miss detection rate is given by

$$\begin{aligned} \beta &= \mathcal{P} [P_a |h_{aw}|^2 + P_b |h_{bw}|^2 + \sigma_w^2 < \tau] \\ &= \begin{cases} 0, & \tau < \sigma_w^2, \\ \mathcal{P} \left[P_b < \frac{\tau - \sigma_w^2 - Q |h_{aw}|^2 / |h_{ab}|^2}{|h_{bw}|^2} \right], & \sigma_w^2 \leq \tau \leq \nu, \\ \mathcal{P} \left[\frac{|h_{aw}|^2}{|h_{ab}|^2} < \frac{\tau - \sigma_w^2 - P_b |h_{bw}|^2}{Q} \right], & \tau > \nu, \end{cases} \\ &= \begin{cases} 0, & \tau < \sigma_w^2, \\ \int_0^{+\infty} \int_0^{\frac{(\tau - \sigma_w^2)z}{Q}} \int_0^{\frac{\tau - \sigma_w^2 - Qy/z}{|h_{bw}|^2}} f_{P_b}(x) f_{|h_{aw}|^2}(y) f_{|h_{ab}|^2}(z) dx dy dz, & \sigma_w^2 \leq \tau \leq \nu, \\ \int_0^{P_b^{\max}} \int_0^{+\infty} \int_0^{\frac{(\tau - \sigma_w^2 - z |h_{bw}|^2)y}{Q}} f_{|h_{aw}|^2}(x) f_{|h_{ab}|^2}(y) f_{P_b}(z) dx dy dz, & \tau > \nu, \end{cases} \\ &= \begin{cases} 0, & \tau < \sigma_w^2, \\ \int_0^{+\infty} \int_0^{\frac{(\tau - \sigma_w^2)z}{Q}} \int_0^{\frac{\tau - \sigma_w^2 - Qy/z}{|h_{bw}|^2}} \frac{\exp\left\{-\left(\frac{y}{\lambda_{aw}} + \frac{z}{\lambda_{ab}}\right)\right\}}{\lambda_{aw} \lambda_{ab} P_b^{\max}} dx dy dz, & \sigma_w^2 \leq \tau \leq \nu, \\ \int_0^{P_b^{\max}} \int_0^{+\infty} \int_0^{\frac{(\tau - \sigma_w^2 - z |h_{bw}|^2)y}{Q}} \frac{\exp\left\{-\left(\frac{x}{\lambda_{aw}} + \frac{y}{\lambda_{ab}}\right)\right\}}{\lambda_{aw} \lambda_{ab} P_b^{\max}} dx dy dz, & \tau > \nu, \end{cases} \\ &= \begin{cases} 0, & \tau < \sigma_w^2, \\ \int_0^{+\infty} \int_0^{\frac{(\tau - \sigma_w^2)z}{Q}} \frac{(\tau - \sigma_w^2 - Qy/z) \exp\left\{-\left(\frac{y}{\lambda_{aw}} + \frac{z}{\lambda_{ab}}\right)\right\}}{\lambda_{aw} \lambda_{ab} P_b^{\max} |h_{bw}|^2} dy dz, & \sigma_w^2 \leq \tau \leq \nu, \\ \int_0^{P_b^{\max}} \int_0^{+\infty} \frac{\left(1 - \exp\left(-\frac{(\tau - \sigma_w^2 - z |h_{bw}|^2)y}{Q \lambda_{aw}}\right)\right) \exp\left(-\frac{y}{\lambda_{ab}}\right)}{\lambda_{ab} P_b^{\max}} dy dz, & \tau > \nu, \end{cases} \end{aligned}$$

$$= \begin{cases} 0, & \tau < \sigma_w^2, \\ \int_0^{+\infty} \frac{((\tau - \sigma_w^2)z + Q\lambda_{aw}) \left(\exp\left(-\frac{(\tau - \sigma_w^2)z}{Q\lambda_{aw}}\right) - 1 \right) \exp\left(-\frac{z}{\lambda_{ab}}\right)}{\lambda_{ab} P_b^{\max} |h_{bw}|^2 z} dz, & \sigma_w^2 \leq \tau \leq \nu, \\ \int_0^{P_b^{\max}} \frac{(\tau - \sigma_w^2 - z|h_{bw}|^2)\lambda_{ab}}{(\tau - \sigma_w^2 - z|h_{bw}|^2)\lambda_{ab} + Q\lambda_{aw}} dz, & \tau > \nu. \end{cases} \quad (43)$$

Following (43), we achieve the desired result in (40) after some algebra manipulations. \blacksquare

We note that the false alarm and miss detection rates derived in Theorem 2 are for an arbitrary detection threshold τ . In practice, Willie will determine the optimal detection threshold that minimizes the detection error probability, which is derived in the following theorem.

Proposition 4: For the decision rule given in (38), Willie's optimal threshold that minimizes the detection error probability is derived as

$$\tau^* = \nu, \quad (44)$$

and the corresponding minimum detection error probability is given by

$$\xi^*(|h_{bw}|^2, t) = 1 - \frac{\lambda_{aw}}{t\lambda_{ab}|h_{bw}|^2} \ln \left(1 + \frac{t\lambda_{ab}|h_{bw}|^2}{\lambda_{aw}} \right). \quad (45)$$

where $t \triangleq P_b^{\max}/Q$ and we recall that $\nu = P_b^{\max}|h_{bw}|^2 + \sigma_w^2$ as defined in (41).

Proof: Following (39) and (40), the detection error probability at Willie is given by

$$\xi = \begin{cases} 1, & \tau < \sigma_w^2, \\ 1 - \frac{Q\lambda_{aw}}{P_b^{\max}|h_{bw}|^2\lambda_{ab}} \ln \left(1 + \frac{(\tau - \sigma_w^2)\lambda_{ab}}{Q\lambda_{aw}} \right), & \sigma_w^2 \leq \tau \leq \nu, \\ 1 - \frac{Q\lambda_{aw}}{P_b^{\max}|h_{bw}|^2\lambda_{ab}} \ln \left(1 + \frac{P_b^{\max}|h_{bw}|^2}{\tau + Q\lambda_{aw}/\lambda_{ab} - \nu} \right), & \tau > \nu. \end{cases} \quad (46)$$

We first note that $\xi = 1$ is the worst case scenario for Willie and thus Willie does not set $\tau < \sigma_w^2$. As per (46), for $\sigma_w^2 \leq \tau \leq \nu$ the detection error probability ξ is a monotonically decreasing function of τ . Thus, Willie will set ν as the threshold to minimize ξ in this case. For $\tau > \nu$, ξ is an monotonically increasing function of τ based on (46), which indicates that Willie will try to set ν as the threshold again to minimize ξ under this case. We also note that for the two cases, i.e., $\sigma_w^2 \leq \tau \leq \nu$ and $\tau > \nu$, setting $\tau = \nu$ can achieve the same detection error probability. As such, we can conclude that the optimal detection threshold is τ . \blacksquare

Following Theorem 2 and Proposition 4, we note that although the noise power at Willie i.e., σ_w^2 appears in the expressions of the false alarm rate, miss detection rate, and the optimal

detection threshold, it does not affect the minimum detection error probability, ξ^* , at Willie. This is due to the fact that Willie knows σ_w^2 and thus he can adjust the optimal detection threshold accordingly to counteract the impact of σ_w^2 . We also note that for $\tau^* = \nu$ the false alarm rate is zero, which means that Willie adjusts the detection threshold to force the false alarm rate being zero in order to minimize the detection error probability. This is achievable, since as assumed Willie knows the value range of Bob's transmit power of the AN signal (i.e., the maximum value of P_b , which is P_b^{\max}).

C. Optimization of Effective Covert Rate

In this subsection, we examine the maximum ECR achieved in the considered scenario with the full-duplex Bob subject to a certain covert communication constraint. In this scenario, Willie knows h_{bw} , which is the reason that the detection performance (e.g., false alarm rate, miss detection rate, optimal detection threshold, and the minimum detection error probability) at Willie depends on h_{bw} . However, Alice does not know h_{bw} and thus cannot guarantee the minimum detection error probability ξ^* being larger than $1 - \epsilon$ as the covert communication constraint. As such, in the following proposition we derive the expected value of ξ^* over all realizations of h_{bw} , which is denoted by $\overline{\xi^*}$, and then we use $\overline{\xi^*} \geq 1 - \epsilon$ as the covert communication constraint in this section.

Proposition 5: The expected value of the minimum detection error probability ξ^* over all realizations of h_{bw} is derived as

$$\begin{aligned} \overline{\xi^*(t)} = 1 - \frac{1}{4\varphi(t)} & \left\{ -\frac{8}{\varphi(t)} {}_3F_3 \left([1, 1, 1], [2, 2, 2], \frac{1}{\varphi(t)} \right) + 4\varsigma \text{Ei} \left(-\frac{1}{\varphi(t)} \right) + \right. \\ & \left. 4 \ln(\varphi(t)) \left(-\text{Ei} \left(-\frac{1}{\varphi(t)} \right) - \frac{\ln(\varphi(t))}{2} + \varsigma \right) + \pi^2 - 2\varsigma^2 - 2 \right\}, \end{aligned} \quad (47)$$

where $\varphi(t) \triangleq t\lambda_{ab}\lambda_{bw}/\lambda_{aw}$, ${}_3F_3([\cdot, \cdot, \cdot], [\cdot, \cdot, \cdot], \cdot)$ is Gauss hypergeometric functions, $\text{Ei}(\cdot)$ is exponential integral function, and ς is the Euler constant.

Proof: Following (45), the expected value of $\xi^*(, t)$ with respect with $|h_{bw}|^2$ is given by

$$\overline{\xi^*(t)} = \int_0^\infty \xi^*(x, t) \frac{e^{-\frac{x}{\lambda_{bw}}}}{\lambda_{bw}} dx$$

$$= 1 - \int_0^\infty \frac{\lambda_{aw}}{xt\lambda_{ab}} \ln \left(1 + \frac{xt\lambda_{ab}}{\lambda_{aw}} \right) \frac{e^{-\frac{x}{\lambda_{bw}}}}{\lambda_{bw}} dx, \quad (48)$$

and solving this integral leads to the desired result in (45). \blacksquare

The optimization problem at Alice of maximizing the ECR subject to a certain covert communication constraint is given by

$$\begin{aligned} Q^* &= \operatorname{argmax}_Q R_c \\ \text{s. t. } &\overline{\xi^*(t)} \geq 1 - \epsilon. \end{aligned} \quad (49)$$

We next determine the solution to the optimization problem given in (49) and derive the maximum ECR in the following theorem.

Theorem 3: For given P_b^{\max} and ϵ , the solution to (49), i.e., the optimal value of Q that maximizes the ECR R_c subject to $\overline{\xi^*(t)} \geq 1 - \epsilon$, is derived as

$$Q^* = P_b^{\max}/t_\epsilon, \quad (50)$$

and the achieved maximum ECR is given by

$$R_c^* = R(1 - e^{-\eta^*} + \eta^* \operatorname{Ei}(-\eta^*)), \quad (51)$$

where t_ϵ is the solution to $\overline{\xi^*(t)} = 1 - \epsilon$ of t and η^* is given by

$$\eta^* = \frac{Q^* - (2^R - 1)\sigma_b^2}{(2^R - 1)\lambda_{bb}\phi P_b^{\max}}. \quad (52)$$

Proof: As per Corollary 1, the transmission outage probability δ is a monotonically decreasing function of Q , which leads to the fact that the ECR R_c monotonically increases with Q . Following this fact, we next prove another fact that the expected minimum detection error probability $\overline{\xi^*(t)}$ is a monotonically increasing function of Q . These two facts indicate that the optimal value of Q (i.e., the solution to (49)) is the one that ensures $\overline{\xi^*(t)} = 1 - \epsilon$. To this end, we next prove that $\overline{\xi^*(t)}$ is a monotonically decreasing function of t , since t is defined as $t = P_b^{\max}/Q \geq 0$. Following (48) and using the Leibniz integral rule, we derive the first derivative of $\overline{\xi^*(t)}$ with respect to t as

$$\frac{\partial \overline{\xi^*(t)}}{\partial t} = \frac{\partial}{\partial t} \left(\underbrace{\int_0^\infty \xi^*(x, t) \frac{e^{-\frac{x}{\lambda_{bw}}}}{\lambda_{bw}} dx}_{\overline{\xi^*(t)}} \right) = \int_0^\infty \frac{\partial \xi^*(x, t)}{\partial t} \frac{e^{-\frac{x}{\lambda_{bw}}}}{\lambda_{bw}} dx. \quad (53)$$

Considering $e^{-\frac{x}{\lambda_{bw}}}/\lambda_{bw} > 0$ in (53), we could conclude that $\partial \overline{\xi^*(t)}/\partial t > 0$ if we could prove $\partial \xi^*(x, t)/\partial t > 0$. Following (45), we have

$$\frac{\partial \xi^*(x, t)}{\partial t} = \frac{g(t)}{t^2(1 + \theta t)}, \quad (54)$$

where

$$g(t) \triangleq \theta(1 + \theta t) \ln(1 + \theta t) - \theta^2 t, \quad (55)$$

and $\theta \triangleq \lambda_{aw}/(x\lambda_{ab}) = \lambda_{aw}/(\lambda_{ab}|h_{bw}|^2) > 0$. We note that the sign of $\partial \xi^*(x, t)/\partial t$ depends on the value of $g(t)$. In order to determine the value range of $g(t)$, we first derive the first derivative of $g(t)$ with respect to t as

$$\frac{\partial g(t)}{\partial t} = \theta^2 \ln(1 + t) > 0. \quad (56)$$

Noting $g(0) = 0$ and following (56), we can conclude that $g(t) \geq 0$, which indicates that $\partial \xi^*(x, t)/\partial t \geq 0$ and thus $\partial \overline{\xi^*(t)}/\partial t \geq 0$. This completes the proof of this theorem. ■

Corollary 2: As Bob's transmit power of the AN signal approaches infinity (i.e., $P_b^{\max} \rightarrow \infty$), the achievable maximum ECR approaches a fixed value, which is given by

$$\lim_{P_b^{\max} \rightarrow \infty} \overline{R}_c^* = R \left(1 - \exp \left(-\frac{1}{(2^R - 1)\lambda_{ab}\phi t_\epsilon} \right) + \frac{\text{Ei} \left(-\frac{1}{(2^R - 1)\lambda_{ab}\phi t_\epsilon} \right)}{(2^R - 1)\lambda_{ab}\phi t_\epsilon} \right). \quad (57)$$

Proof: As per (45) and (47), we note that the solution of t to $\overline{\xi^*(t)} = 1 - \epsilon$ does not affect by the value of P_b^{\max} . As such, we still have t_ϵ as the solution to $\overline{\xi^*(t)} = 1 - \epsilon$ as $P_b^{\max} \rightarrow \infty$. Then, substituting $Q^* = P_b^{\max}/t_\epsilon$ into (52) we have

$$\lim_{P_b^{\max} \rightarrow \infty} \eta^* = \frac{1}{(2^R - 1)\lambda_{bb}\phi t_\epsilon}. \quad (58)$$

Then, substituting (58) into (51) we achieve the desired result in (57) after some algebra manipulations. ■

We note that increasing Bob's transmit power of the AN signal increases the amount of uncertainty and thus increases the detection error probability at Willie. However, the increase in Bob's transmit power of the AN signal also leads to more self-interference at Bob due to the non-zero ϕ . This intuitively explains the result presented in Corollary 2, which indicates that increasing Bob's transmit power of the AN signal above some specific value does not bring in extra benefit in terms of increasing the achievable maximum ECR.

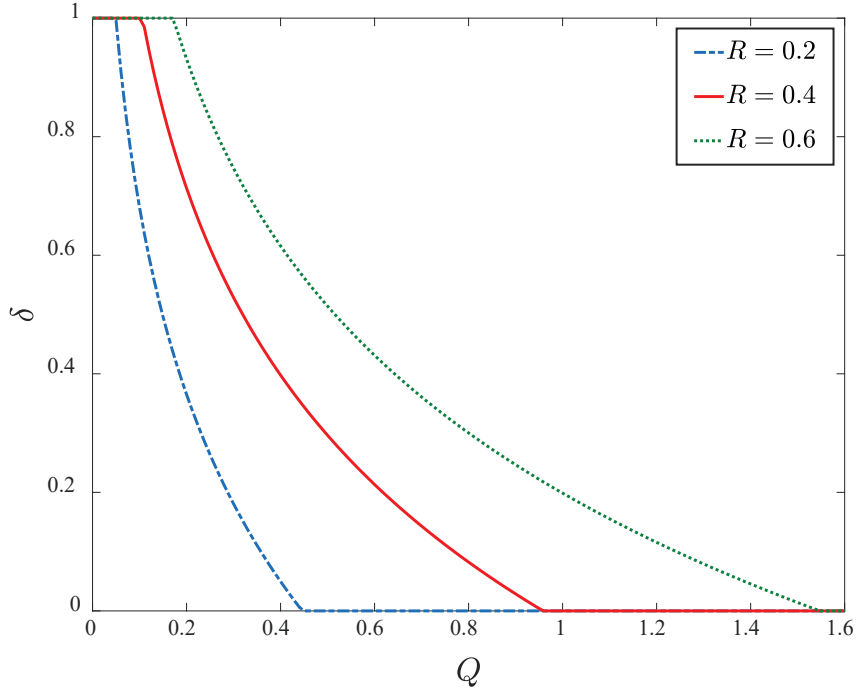


Fig. 2. Transmission outage probability from Alice to Bob (δ) versus Q with different values of R , where $\hat{\sigma}_b^2 = 0$ dB and $\rho_b = 3$.

V. NUMERICAL RESULTS

In this section, we first present numerical results to verify our analysis on the covert communications in the considered two scenarios (i.e., with noise uncertainty and with the full-duplex Bob). Then, we provide a thorough performance examination of the covert communications in each scenario. Based on our examination, we draw many useful insights and guidelines on how to design and implement covert communications in practical scenarios.

A. Covert Communication with Noise Uncertainty

In Fig. 2, we plot the transmission outage probability from Alice to Bob (i.e., δ) versus Q with different values of R . In this figure, we first observe that δ monotonically decreases with Q for a fixed transmission rate R , since a larger Q requires a higher transmit power at Alice. As expected, we also observe that δ increases as the fixed transmission rate R increases.

Fig. 3 illustrates the false alarm rate α , miss detection rate β , and detection error probability ξ versus Willie's detection threshold τ . As expected, we first observe that the simulated curves

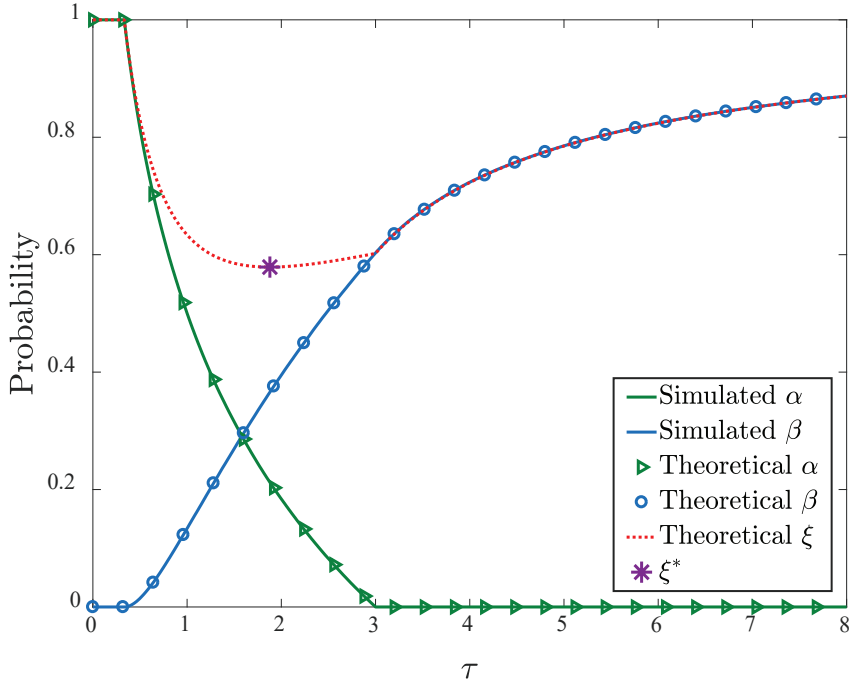


Fig. 3. Willie's false alarm rate α , miss detection rate β , and detection error probability ξ versus τ for covert communications with the noise uncertainty, where $Q = 1$, $\rho_w = 3$, $\hat{\sigma}_w^2 = 0$ dB, and $\lambda_{ab} = \lambda_{aw} = 1$.

precisely match the theoretical ones, which confirms the correctness of our Theorem 1. We also observe that there indeed an optimal value of τ that minimizes ξ and this value satisfies $\hat{\sigma}_w^2/\rho \leq \tau^* \leq \rho\hat{\sigma}_w^2$, which verifies the correctness of our Proposition 2.

In Fig. 4, we plot the maximum ECR R_c^* versus the noise uncertainty parameter at both Bob and Willie with different levels of covert communication constraints (i.e., different values of ϵ), where we set $\rho_b = \rho_w = \rho$. In this figure, we observe that R_c^* first increases then decreases as ρ increases, which indicates that there is a value of ρ that maximizes R_c^* . This can be explained by the fact that the noise uncertainty simultaneously increases the detection error probability at Willie and the transmission outage probability from Alice to Bob, which means that the noise uncertainty has a two-side impact on covert wireless communications. As expected, we also observe that R_c^* increases as the required levels of the covert communication constraint increases (i.e., when ϵ increases), which demonstrates that it is the covert communication constraint that mainly limits the maximum ECR.

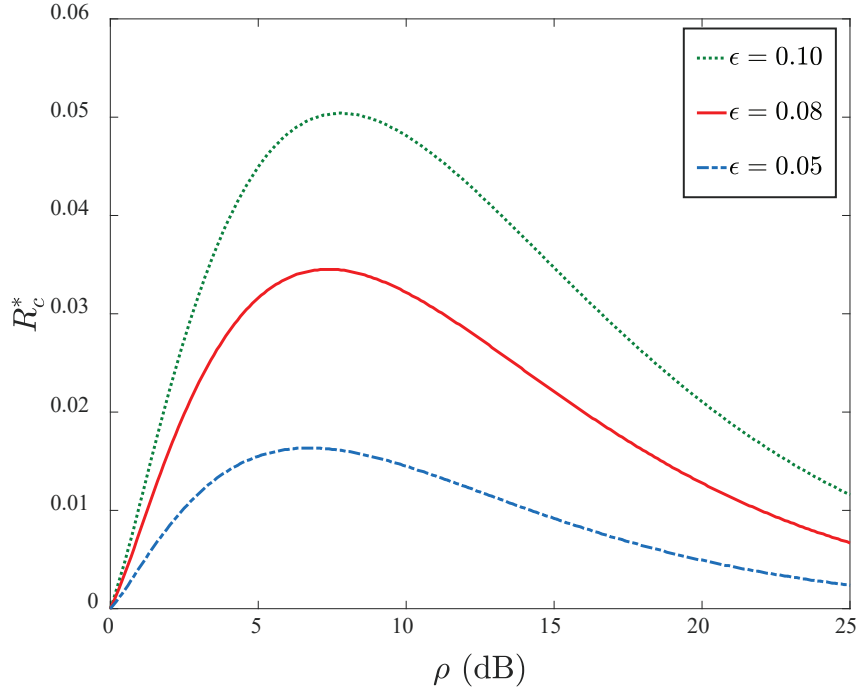


Fig. 4. The maximum ECR R_c^* versus the noise uncertainty parameter ρ with different values of ϵ , where $\hat{\sigma}_b^2 = \hat{\sigma}_w^2 = 0$ dB and $\lambda_{ab} = \lambda_{aw} = 1$.

B. Covert Communications with A Full-Duplex Receiver

In Fig. 5, we plot the transmission outage probability from Alice to Bob (i.e., δ) versus Q with different values of P_b^{\max} . In this figure, We first observe that δ monotonically decreases with Q for a fixed transmission rate R , since a larger Q requires a higher transmit power at Alice. We also observe that δ is a monotonically increasing function of P_b^{\max} , which verifies the correctness of our Corollary 1.

In Fig. 6, we plot the false alarm rate α , miss detection rate β , and detection error probability ξ versus Willie's detection threshold τ in the covert communication scenario with the full-duplex Bob. As expected, in this figure we first observe that the simulated curves precisely match the theoretical ones, which confirms the correctness of our Theorem 2. We also observe that the detection error probability ξ dramatically varies with the detection threshold τ , which demonstrates the necessity of optimizing τ by Willie and the importance of our Proposition 4, which derives the optimal detection threshold minimizes ξ in a closed-form expression. Finally, we observe that the optimal value of τ is equal to ν , which simultaneously forces the false alarm

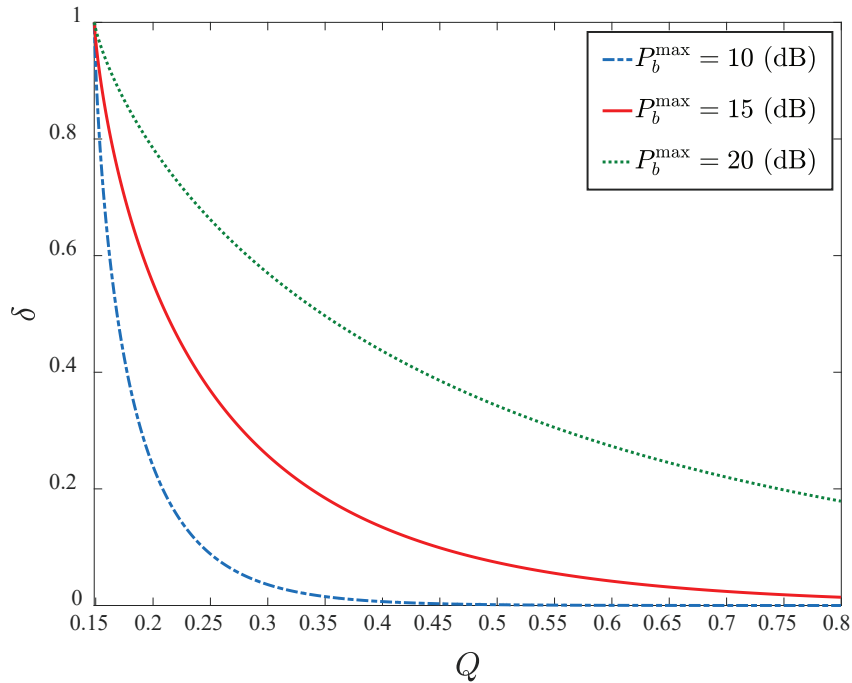


Fig. 5. Transmission outage probability from Alice to Bob (δ) versus Q with different values of P_b^{\max} , where $\hat{\sigma}_w^2 = 0$ dB, $R = 0.2$, and $\phi = 0.05$.

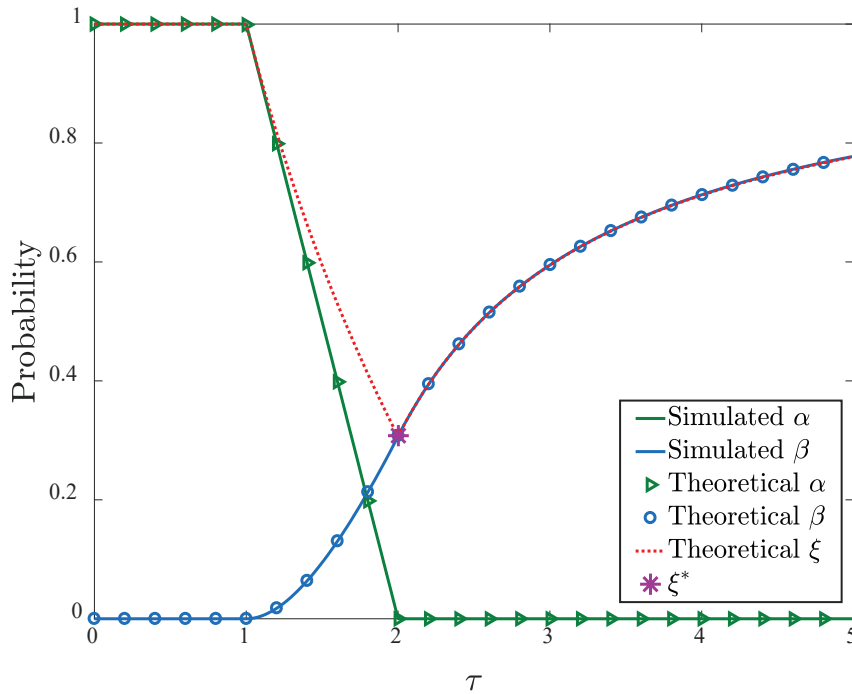


Fig. 6. Willie's false alarm rate α , miss detection rate β , and detection error probability ξ versus τ for covert communications with the full-duplex Bob, where $Q = 1$, $P_b^{\max} = 0$ dB, $|h_{bw}|^2 = 1$, and $\lambda_{ab} = \lambda_{aw} = 1$.

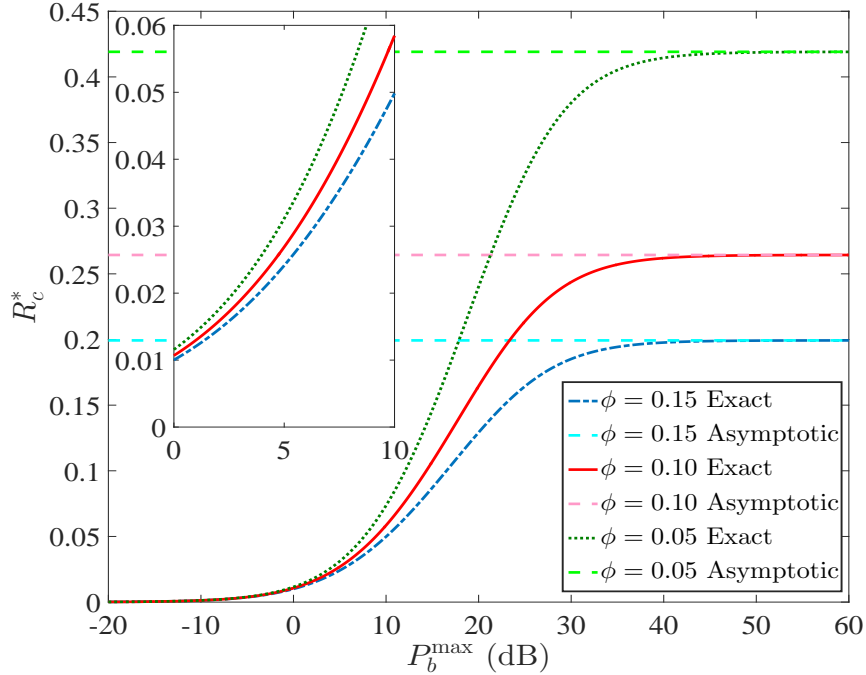


Fig. 7. R_c^* versus P_b^{\max} under different value of ϕ , where $\epsilon = 0.10$, $\sigma_b^2 = 0$ dB, and $\lambda_{ab} = \lambda_{aw} = \lambda_{bb} = \lambda_{bw} = 1$.

rate α at Willie being zero and minimizes the miss detection rate β .

In Fig. 7, we plot the maximum ECR R_c^* versus Bob's maximum transmit power of the AN signal P_b^{\max} with different values of the self-interference cancellation parameter ϕ . In this figure, we first observe that R_c^* monotonically increases as P_b^{\max} increases, which demonstrates that the covert communications from Alice becomes easier when Bob has more power to transmit AN to aid. However, we also note that as $P_b^{\max} \rightarrow \infty$ the maximum ECR R_c^* approaches to the upper bound given in our Corollary 2. Intuitively, this can be explained by the fact that the transmitted AN not only creates interference at Willie but also leads to self-interference at Bob. In this figure, we also observe that the upper bound on the achieved R_c^* decreases significantly as ϕ increases, since a larger ϕ indicates a larger self-interference at Bob. Comparing the results in Fig. 4 and Fig. 7, we can see that the full-duplex Bob can aid to achieve a larger ECR than the noise uncertainty, as long as the self-interference at Bob can be effectively cancelled (e.g., when $\phi \leq 0.1$).

VI. CONCLUSION

This work examined covert communications with noise uncertainty or a full-duplex receiver over Rayleigh fading channels, in which the transmitter Alice adopts the channel inversion power control to transmit information to the receiver Bob covertly while trying to hide herself from the warden Willie. We analyzed Willie's detection performance limits in terms of the detection error probability, based on which we determined the achievable ECRs. Our examination shows that there exists a certain amount of noise uncertainty that can maximize the ECR. With the full-duplex receiver Bob, the ECR monotonically increases and approaches to an upper bound as the maximum power at Bob of the AN signal increases. Our analysis and examinations provided practical guidelines on conducting covert communications and potentially hiding a transmitter in Rayleigh fading scenarios.

REFERENCES

- [1] A. Mukherjee, "Physical-layer security in the internet of things: Sensing and communication confidentiality under resource constraints," *Proceedings of the IEEE*, vol. 103, no. 10, pp. 1747–1761, Oct. 2015.
- [2] Q. Xu, P. Ren, H. Song, and Q. Du, "Security enhancement for IoT communications exposed to eavesdroppers with uncertain locations," *IEEE Access*, vol. 4, pp. 2840–2853, Jun. 2016.
- [3] A. J. Menezes, P. C. van Oorschot, and S. A. Vanstone, *Handbook of Applied Cryptography*. CRC Press, 1996.
- [4] J. Talbot and D. Welsh, *Complexity and Cryptography: An Introduction*. Cambridge University Press, 2006.
- [5] S. Rich and B. Gellman, "NSA seeks to build quantum computer that could crack most types of encryption," *The Washington Post*, 2014, [Online]. Available: <http://wapo.st/19DycJT>.
- [6] N. Zhao, F. R. Yu, M. Li, and V. C. Leung, "Anti-eavesdropping schemes for interference alignment (IA)-based wireless networks," *IEEE Trans. Wireless Commun.*, vol. 15, no. 8, pp. 5719–5732, Aug. 2016.
- [7] Y. Deng, L. Wang, S. A. R. Zaidi, J. Yuan, and M. Elkashlan, "Artificial-noise aided secure transmission in large scale spectrum sharing networks," *IEEE Trans. Commun.*, vol. 64, no. 5, pp. 2116–2129, May 2016.
- [8] S. Yan, X. Zhou, N. Yang, B. He, and T. D. Abhayapala, "Artificial-noise-aided secure transmission in wiretap channels with transmitter-side correlation," *IEEE Trans. Wireless Commun.*, vol. 15, no. 12, pp. 8286–8297, Dec. 2016.
- [9] Y. Liu, Z. Qin, M. Elkashlan, Y. Gao, and L. Hanzo, "Enhancing the physical layer security of non-orthogonal multiple access in large-scale networks," *IEEE Trans. Wireless Commun.*, vol. 16, no. 3, pp. 1656–1672, Mar. 2017.
- [10] B. A. Bash, D. Goeckel, and D. Towsley, "Limits of reliable communication with low probability of detection on AWGN channels," *IEEE J. Sel. Areas Commun.*, vol. 31, no. 9, pp. 1921–1930, Sep. 2013.
- [11] P. H. Che, M. Bakshi, and S. Jaggi, "Reliable deniable communication: Hiding messages in noise," in *Proc. IEEE Int. Symp. Inf. Theory*, Jul. 2013, pp. 2945–2949.

- [12] B. A. Bash, D. Goeckel, D. Towsley, and S. Guha, "Hiding information in noise: fundamental limits of covert wireless communication," *IEEE Commun. Mag.*, vol. 53, no. 12, pp. 26–31, Dec. 2015.
- [13] M. Bloch, "Covert communication over noisy channels: A resolvability perspective," *IEEE Trans. Inf. Theory*, vol. 62, no. 5, pp. 2334–2354, May 2016.
- [14] D. Goeckel, B. A. Bash, S. Guha, and D. Towsley, "Covert communications when the warden does not know the background noise power," *IEEE Commun. Lett.*, vol. 20, no. 2, pp. 236–239, Feb. 2016.
- [15] L. Wang, G. W. Wornell, and L. Zheng, "Fundamental limits of communication with low probability of detection," *IEEE Trans. Inf. Theory*, vol. 62, no. 6, pp. 3493–3503, Jun. 2016.
- [16] S. Lee, R. J. Baxley, M. A. Weitnauer, and B. T. Walkenhorst, "Achieving undetectable communication," *IEEE J. Sel. Topics Signal Process.*, vol. 9, no. 7, pp. 1195–1205, Oct. 2015.
- [17] B. He, S. Yan, X. Zhou, and V. K. N. Lau, "On covert communication with noise uncertainty," *IEEE Commun. Lett.*, vol. 21, no. 4, pp. 941–944, Apr. 2017.
- [18] S. Yan, B. He, Y. Cong, and X. Zhou, "Covert communication with finite blocklength in AWGN channels," in *Proc. IEEE ICC*, May 2017, pp. 1–6.
- [19] K. Shahzad, X. Zhou, and S. Yan, "Covert communication in fading channels under channel uncertainty," in *Proc. IEEE VTC Spring*, Jun. 2017, pp. 1–5.
- [20] J. Hu, S. Yan, X. Zhou, F. Shu, J. Li, and J. Wang, "Covert communication in wireless relay networks," in *Proc. IEEE GLOBECOM*, Dec. 2017, pp. 1–6.
- [21] S. Shellhammer and R. Tandra, *Performance of the Power Detector With Noise Uncertainty*. IEEE Std. 802.22-06/0134r0, Jul. 2006.
- [22] R. Tandra and A. Sahai, "SNR walls for signal detection," *IEEE Jour. on Sel. Topics in Signal Process.*, vol. 2, no. 1, pp. 4–17, Feb. 2008.
- [23] S. S. Kalamkar, A. Banerjee, and A. K. Gupta, "SNR wall for generalized energy detection under noise uncertainty in cognitive radio," in *Proc. IEEE 19th Asia Pacific Conf. Commun. (APCC)*, Aug. 2013, pp. 375–380.
- [24] M. H. DeGroot, *Probability and Statistics*, 4th ed. Pearson, 2011.
- [25] J. Hu, K. Shahzad, S. Yan, X. Zhou, F. Shu, and J. Li, "Covert communications with a full-duplex receiver over wireless fading channels," in *Proc. IEEE ICC*, May 2018, pp. 1–6, accepted to appear, arXiv:1711.03684.
- [26] E. Ahmed and A. M. Eltawil, "All-digital self-interference cancellation technique for full-duplex systems," *IEEE Trans. Wireless Commun.*, vol. 14, no. 7, pp. 3519–3532, Jul. 2015.
- [27] E. Everett, A. Sahai, and A. Sabharwal, "Passive self-interference suppression for full-duplex infrastructure nodes," *IEEE Trans. Wireless Commun.*, vol. 13, no. 2, pp. 680–694, Feb. 2014.